Dynamics of conformational transitions to isomeric states favoring intramolecular excimer formation in aromatic polyesters with methylene or oxyethylene spacers

Ivet Bahar and Wayne L. Mattice
Polymer Research Center, Department of Chemical Engineering, Bogazici University, Bebek 80815, Istanbul, Turkey and Institute of Polymer Science, The University of Akron, Akron, Ohio 44325-3909

(Received 3 November 1988; accepted 22 February 1989)

The dynamic rotational isomeric state formalism described in the preceding paper is used to calculate the rate of first passage from non-excimer-forming conformations to excimer-forming conformations in seven aromatic polyesters with different flexible spacers between the aromatic rings. The excimer-forming conformations in these polymers were identified recently by Mendicuti *et al.* The time dependence of the probability that a flexible spacer will at least once have passed through an excimer-forming conformation can be written as the product of two factors, one of which is time dependent, the other of which is determined by the equilibrium conformational statistics. In the polyesters considered here, the static factor is much more sensitive than the dynamic factor to the identity of the flexible spacers. Consequently, the equilibrium chain statistics provides a good description of the relative excimer population for these polyesters, even at times where the dynamic contribution is significant. The chromophores in these polyesters have such short fluorescence lifetimes that it is only in the most mobile flexible segments that there is an important dynamic contribution to the excimer formation.

I. INTRODUCTION

In the preceding paper,[1] a stochastic model is developed to determine the time-dependent increase in the fraction of polymeric segments that enter the macrostate $\{\phi\}_a$, during the time interval $(0,t)$. The macrostate $\{\phi\}_a$ consists of the conformations that favor excimer emission, i.e., those conformations that place the chromophoric groups at the termini of the N mobile bonds (with ν states available to each) parallel to each other with a separation of about 3 Å. The macrostate $\{\phi\}_b$ comprises all conformations which do not fulfill this requirement. The mean first passage time $\langle\tau\rangle$ from macrostate $\{\phi\}_b$ to macrostate $\{\phi\}_a$ plays an important role in determining the contribution of conformational transitions to excimer formation. If the residence time of the singlet excitation on a particular chromophore at a non-excimer-forming site is long enough compared to $\langle\tau\rangle$, significant rotational sampling of conformations leading to excimer formation may occur. If, on the other hand, the residence time is much shorter than $\langle\tau\rangle$, only sites formed prior to excitation can form excimers. In this case the efficiency of excimer emission is governed by the equilibrium statistics of the chain. The strong excimer emission observed in meso dyads in polystyrene is asserted to be of dynamic origin,[2] as the preceding work confirms.

Recent experiments[3,4] with polyesters with different sizes of flexible spacers between the aromatic groups demonstrate a close correlation between the intensity of intramolecular excimer emission and the equilibrium probability of occurrence of conformations favoring excimer formation. However, in general, if conformational transitions to states conducive to excimer emission are fast enough, in the sense that they take place before the excited chromophore deactivates by some other mechanism, the observed spectra should depend not only on the equilibrium population of segments favoring excimer formation, but also on the extent of the dynamic contribution to increase the number of such segments. As an attempt to estimate the relative contribution of the static and dynamic factors, the increase with time in the population of excimer-forming conformations is theoretically analyzed in the present work, using the dynamic rotational isomeric states formulation. A rigorous mathematical scheme for calculating the latter was presented in the preceding paper.[1] An approximate method, based on the description of the excimer-sampling process as a two-state Markov process, will be preferred in the present study, due to the large number of microstates (conformations) in each macrostate.

A brief outline of the theoretical approach adopted in the present work is given in the next section. The purpose is to estimate $\langle\tau\rangle$ for the different segments considered, from the analysis of the dynamics of the stationary process of conformational transitions in the ensemble of polymeric segments in equilibrium.

The polyesters considered in the present study are classified in two series. Series I consists of polymers with repeating unit p-OC–C_6H_5COO–$(CH_2CH_2O)_m$– where m is varied from 1 to 3. Series II refers to polymers with repeating unit p-OC–C_6H_5COO–$(CH_2)_x$O– with $x = 2$–6. The member of series I for which $m = 1$ is identical with the member of series II for which $x = 2$. The conformations that give rise to excimer formation in these polymers were identified recently.[3,4] They are characterized by a set of torsional angles corresponding to each mobile bond between the rings, following the conventional rotational isomeric states (RIS) model.[5] The set of such conformations composes the macrostate $\{\phi\}_a$ for each segment considered. Their equilibrium probabilities were estimated[3,4] from previous conforma-

 0021-9606/89/116783-08$02.10

tional energy analysis by Riande and collaborators,[6] and by Abe and Mark.[7] The analysis of local chain dynamics necessitates, however, knowledge of not only the energy parameters at the isomeric minima, but also the heights of the saddles between them. In the treatment below, which is based on the dynamic RIS model,[8] the rates of transitions between isomeric states are represented by Arrhenius type expressions with activation energies equal to the barrier heights to be crossed. Therefore the conformational characteristics of each mobile pair of bonds in the two series is reinvestigated to extract the required data on the barrier heights. Calculations are presented in Sec. III, which is followed by the results and discussion section. The dynamic RIS model is employed in the calculations to determine the time-dependent transition probability $P(a/b)$ for the passage from $\{\phi\}_b$ to $\{\phi\}_a$ in the stationary process. This transition probability is used to estimate the corresponding first passage times.

II. THEORY

The transition from one macrostate to another for a given segment is approximated by a two-state Markov process

$$\{\phi\}_a \underset{\lambda}{\overset{\mu}{\rightleftarrows}} \{\phi\}_b,$$

where λ and μ refer to the indicated mean rates of passage.[9] Macrostates $\{\phi\}_a$ and $\{\phi\}_b$ comprise, in turn, several microstates. ϕ_i refers to the ith microstate. Let $P(a/b)$ be the transition or conditional probability of occurrence of macrostate $\{\phi\}_a$ at time t, given macrostate $\{\phi\}_b$ at $t=0$. Similar definitions hold for $P(a/a)$, $P(b/b)$, and $P(b/a)$. The transition probabilities satisfy the Kolmogorov differential equations[9]

$$\begin{aligned}
\frac{dP(a/a)}{dt} &= -\mu P(a/a) + \lambda P(b/a), \\
\frac{dP(b/a)}{dt} &= -\lambda P(b/a) + \mu P(a/a), \\
\frac{dP(b/b)}{dt} &= -\lambda P(b/b) + \mu P(a/b), \\
\frac{dP(a/b)}{dt} &= -\mu P(a/b) + \lambda P(b/b),
\end{aligned} \tag{1}$$

which may be solved to find

$$P(a/a) = \lambda/(\lambda+\mu) + [\mu/(\lambda+\mu)]\exp[-(\lambda+\mu)t], \tag{2}$$

$$P(a/b) = \lambda(\lambda+\mu)^{-1}\{1-\exp[-(\lambda+\mu)t]\} \tag{3}$$

and

$$P(b/a) = 1 - P(a/a), \tag{4}$$

$$P(b/b) = 1 - P(a/b). \tag{5}$$

The asymptotic limits that the above transition probabilities approach as t goes to infinity are the equilibrium probabilities of the macrostates, i.e.,

$$P^0(a) = \lambda/(\lambda+\mu), \tag{6}$$

$$P^0(b) = \mu/(\lambda+\mu). \tag{7}$$

The above equations describe a stationary process where all transitions are counterbalanced by back transitions. In mathematical terms, we have

$$P(a/b)P^0(b) = P(b/a)P^0(a) \tag{8}$$

which is a direct consequence of the principle of detailed balance for the ensemble of polymeric chains in equilibrium. The superscript 0 refers to quantities dictated by the equilibrium statistics of the chain. Thus the instantaneous probability $P'(a)$ or $P'(b)$ of a given macrostate, or equivalently the fraction of segments with conformations belonging to those macrostates, will be constant and equal to the equilibrium value $P^0(a)$ or $P^0(b)$, as may be easily shown by inserting Eqs. (8) and (4) into the general expression

$$P'(a) = P(a/a)P^0(a) + P(a/b)P^0(b). \tag{9}$$

The above description gives no information about the accumulation in the number of segments which has undergone transition to an excimer-forming conformation before reaching time t. In fact, the quantity of interest is the fraction of segments which has passed through the macrostate $\{\phi\}_a$ at least once during the time interval $(0,t)$. This quantity may be evaluated by considering an irreversible hypothetical process where back transitions from $\{\phi\}_b$ to $\{\phi\}_a$ are precluded, as carried out in the preceding paper. Thus, in the new process, $\mu = 0$, or

$$P_n(a/a) = 1, \tag{10}$$

$$P_n(a/b) = 1 - \exp(-\lambda_n t). \tag{11}$$

Here the subscripts n are appended to distinguish the quantities associated with the nonequilibrium irreversible process from those corresponding to the stationary process. Clearly, $P_n(a/b)$ converges to one, at long times, in contrast to $P(a/b)$ of the stationary process, which approaches $P^0(a)$. Another way of stating the same property is

$$\int_0^\infty \dot{P}(a/b)dt = P^0(a) \tag{12}$$

and

$$\int_0^\infty \dot{P}_n(a/b)dt = 1, \tag{13}$$

where the upper dots indicate the time derivative.

The mean rate of passage λ_n from $\{\phi\}_b$ to $\{\phi\}_a$ in the new irreversible process may be estimated from the equilibrium $P(a/b)$ curve using the following initial condition. At $t=0$, the probability distribution of configurations is prescribed by equilibrium statistics. The condition of $\lambda_n = \lambda$ is imposed starting from $t=0$, i.e., in the limit as $t\to 0$, $P_n(a/b)$ should be identical to $P(a/b)$. More precisely, their time derivatives $\dot{P}_n(a/b)$ and $\dot{P}(a/b)$ are equal to each other at $t=0$. A rough sketch of the transition probabilities and their time derivatives for the two processes is given in Fig. 1. Thus, the mean rate λ_n will be determined from the initial slope of the $P(a/b)$ curve of the stationary process, as

$$\lambda_n = \dot{P}(a/b)|_{t=0} \tag{14}$$

and will be inserted in Eq. (11), to evaluate $P_n(a/b)$. Although Eq. (11) is a rather simple one, it may conveniently be used as a first-order approximation to estimate and compare the relative contribution of local chain dynamics to ex-

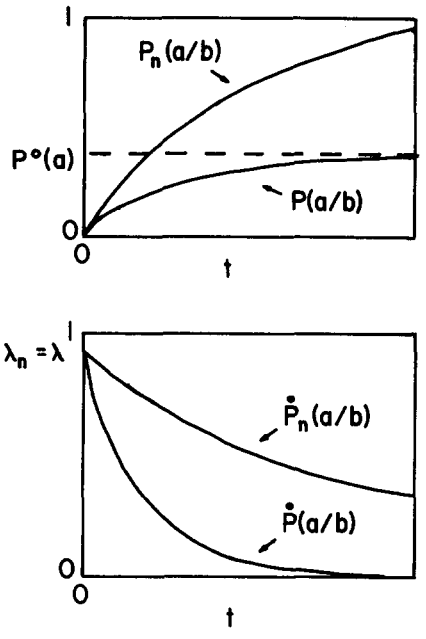

FIG. 1. (Top panel) Time dependence of the transition probabilities $P(a/b)$ and $P_n(a/b)$ for the stationary and nonequilibrium processes, respectively. $P(a/b)$ converges to the equilibrium probability $P^0(a)$ of macrostate $\{\phi\}_a$. $P_n(a/b)$ approaches one. (Bottom panel) Decay of the rates of transition probabilities with time. Both curves intersect the abscissa at $\dot{P}(a/b) = \dot{P}_n(a/b) = \lambda = \lambda_n$.

cimer formation in different members of the series of polyesters.

By differentiating both sides of Eq. (8) with respect to time, we obtain

$$\dot{P}(a/b) = \dot{P}(b/a)P^0(a)/P^0(b). \tag{15}$$

On the other hand, from Eq. (4) we have

$$\dot{P}(b/a) = -\dot{P}(a/a). \tag{16}$$

Equations (15) and (16) are valid both for the stationary and the nonequilibrium process at $t = 0$. Their substitution into Eq. (14) yields

$$\lambda_n = -\dot{P}(a/a)|_{t=0}[P^0(a)/P^0(b)]. \tag{17}$$

The use of Eq. (17) offers two important advantages in this work. First, the time required to compute $\dot{P}(a/a)$ is considerably lower compared to the other transition probabilities, due to the smaller number of conformations over which summations have to be performed (see sequel). Another advantage Eq. (17) offers is that the mean rate of passage from $\{\phi\}_b$ to $\{\phi\}_a$ is expressed as the product of two terms, reflecting the influence of chain dynamics and equilibrium statistics, separately. In fact, the first term describes how fast a conformation which is initially in macrostate $\{\phi\}_a$ tends to quit this macrostate. This rate is related to the mobility of the chain and will be found to be larger in relatively longer sequences which enjoy a higher degree of orientational freedom, provided that a mean friction coefficient is adopted in the rate expressions, regardless of the size of the mobile group. As to the term in brackets in Eq. (17), it is clearly governed by equilibrium statistics. By evaluating the rate λ_n according to Eq. (17), it will be possible to realize which factor predominantly determines the observed behavior.

The mean first passage time from $\{\phi\}_b$ to $\{\phi\}_a$ is found from

$$\langle\tau\rangle \equiv \int_0^\infty [1 - P_n^t(a)]\,dt = P^0(b)/\lambda_n \tag{18}$$

as follows from

$$P_n^t(a) = P^0(a) + [1 - \exp(-\lambda_n t)]P^0(b) \tag{19}$$

which gives the time-dependent increase in the fraction of segments conducive to excimer emission.

III. CALCULATIONS

A. Conformational energies

Energy calculations are carried out, as usual, for the central bond pair in a six-bond unit, the rotational states of the bonds next to the pair being held in the *trans* position. Three contributions, the intrinsic threefold torsional potential, the van der Waals interaction, and the electrostatic interaction, are summed up according to

$$E(\phi_i, \phi_{i+1}) = E(\phi_i) + E(\phi_{i+1}) + \sum_{j,k}[b_{jk}/r_{jk}^{12} - a_{jk}/r_{jk}^6] + \sum_{j,k} k'\delta_j\delta_k/\epsilon r_{jk} \tag{20}$$

with

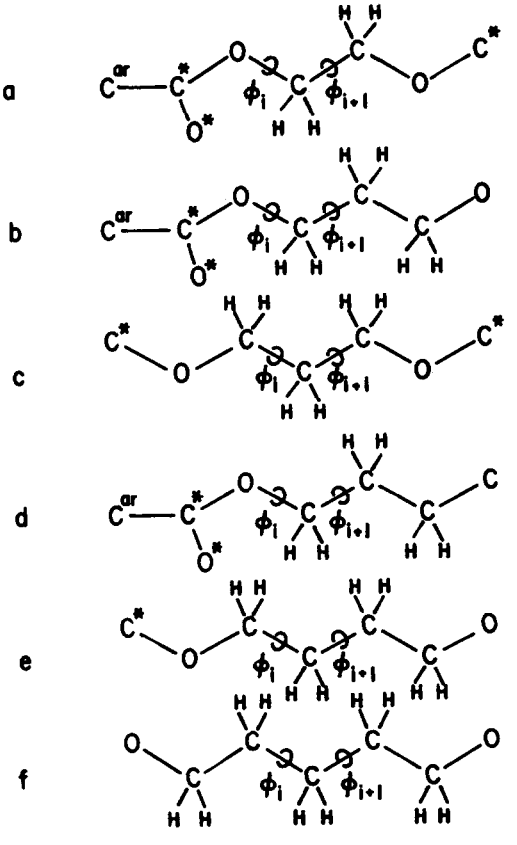

FIG. 2. Schematic representation of the segments in series II considered in conformational energy calculations. The segments belong to the chains with (a) $x = 2$ (or $m = 1$); (b), (c) $x = 3$; (d)–(f) $x = 4$–6.

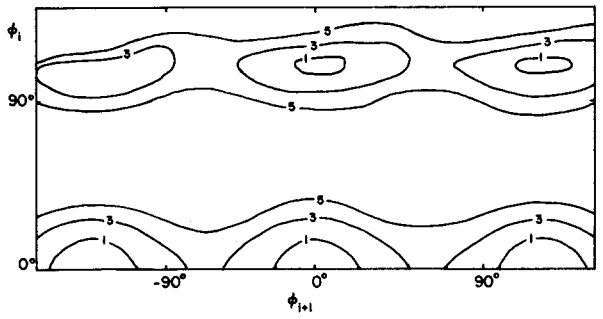

FIG. 3. Conformational energy diagram for segment (a) in Fig. 2. Energy contours are labeled with respect to the *tt* state. Values at the energy minima and saddle points are listed in Tables I and II, respectively.

$$E(\phi_i) = (E_0/2)[1 - \cos 3\phi_i] \tag{21}$$

Here $E(\phi)_i$ represents the torsional potential ascribed to the bond with rotation ϕ_i. E_0 is assigned the values 2.8 and 1.8 kcal/mol for C–C and C–O bonds, respectively, in agreement with previous calculations.[7] The van der Waals interactions are represented by the 6-12 Lennard-Jones equation with parameters a_{jk} and b_{jk} for each pair of nonbonded atoms j and k, separated by a distance r_{jk}. Coulombic interactions are calculated by assigning partial charges δ_j and δ_k to the interacting nonbonded atoms. The conversion factor k' in Eq. (20) equals 332 when r_{jk} is in Å. The value 3 is used for the dielectric constant ϵ. The dispersion parameters a_{ij} are calculated using the Slater–Kirkwood formula,[11] and b_{ij} are chosen so as to minimize the Lennard-Jones potential between atoms j and k when their separation equals the sum of their van der Waals radii. The parameters for the Slater–Kirkwood equation and the geometric parameters are directly taken from the work of Riande *et al.*[10] which yields satisfactory agreement with experiments. Partial electronic charges used in Ref. 7 are adopted in the present study. The effect of the coulombic interaction is found to be small compared to the other contributions.

Figure 2 displays six polymeric segments representative of various pairs of bonds in the chains belonging to series II. The conformational energy maps associated with those segments are given in Figs. 3–8. Only those portions of the maps with ϕ_i varying in the interval (0°, 180°) are shown, due to

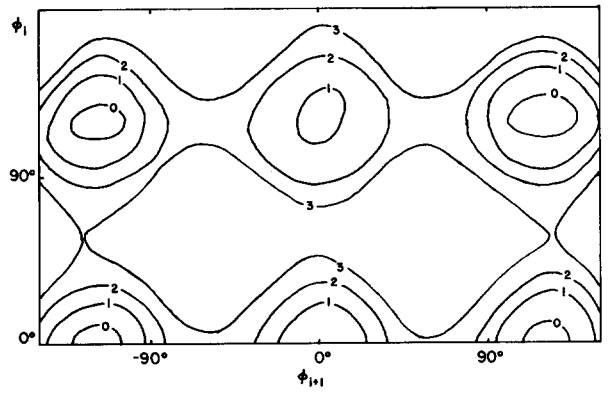

FIG. 4. Conformational energy diagram for segment (b) in Fig. 2. See legend to Fig. 3.

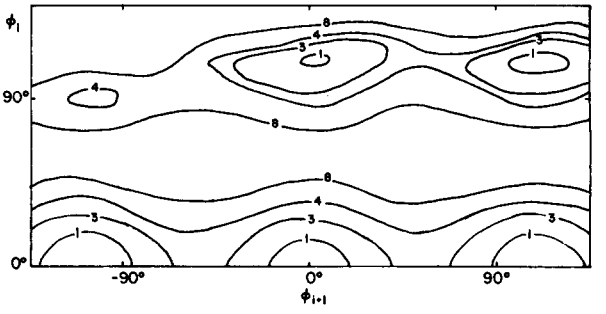

FIG. 5. Conformational energy diagram for segment (c) in Fig. 2. See legend in Fig. 3.

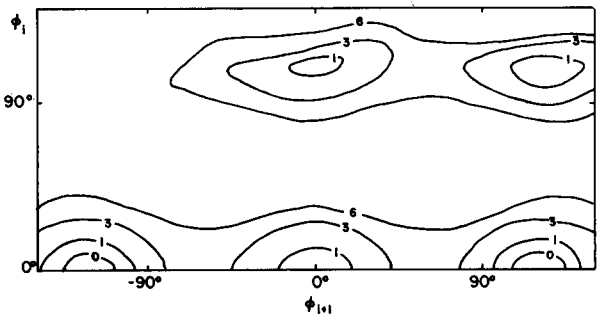

FIG. 6. Conformational energy diagram for segment (d) in Fig. 2. See legend to Fig. 3.

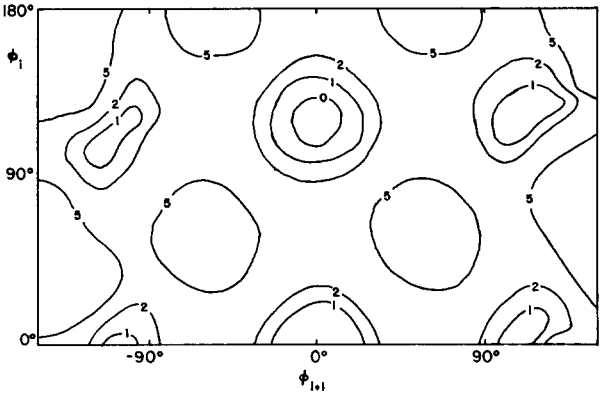

FIG. 7. Conformational energy diagram for segment (e) in Fig. 2. See legend to Fig. 3.

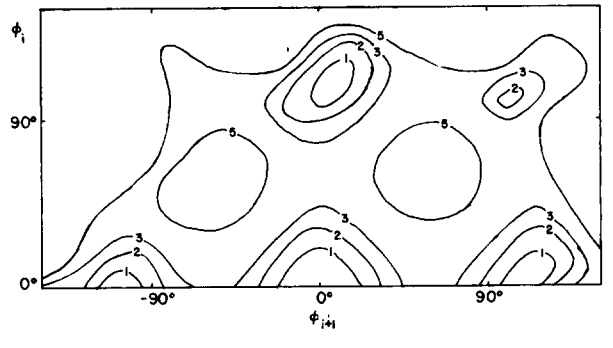

FIG. 8. Conformational energy diagram for segment (f) in Fig. 2. See legend to Fig. 3.

TABLE I. Conformational energies (kcal/mole).[a,b]

Segment	Isomeric states			
	$tg^{\pm}$	$g^{\pm}t$	$g^{\pm}g^{\pm}$	$g^{\pm}g^{\mp}$
1	0	0.7	0.6	1.6
2	−0.4	0.6	0.2	3.4
3	−0.4	−0.4	−0.8	−0.5
4	−0.2	0.4	0.2	11.0
5	0.5	−0.2	0.3	0.85
6	0.5	0.5	1.0	3.0
7	0.9	−0.4	0.5	0.9
8	0.9	0.9	1.8	11.0
9	−0.4	0.4	0	11.0

[a] All values are tabulated with respect to the *tt* state whose conformational energy is set equal to zero.
[b] Segments 1–6 are shown in Figs. 2(a)–2(f). Segments 7 and 8 correspond to the pair of bonds (CC, CO) and (CO, OC) nonadjacent to the terephthalic groups in series I. Segment 9 refers to the pair (OC, CC) adjacent to the terephthalic group in series I.

the symmetry with respect to $(\phi_i, \phi_{i+1}) = (0°, 0°)$. The energy values adopted in the present study for the isomeric minima and saddle heights are listed in Tables I and II, respectively. The equilibrium data recently employed by Mendicuti *et al.*[4] is reproduced by minor adjustment (± 0.2 kcal/mol) of the energy minima for $x = 3$–6. However, values for $x = 2$ are found to considerably deviate from those previously used, which had been adjusted to optimize agreement with experimentally determined conformation-dependent equilibrium properties.[6] Results are almost unchanged when calculations are repeated with longer segments, including the interaction of the neighboring rings. As to the series I, involving ethylene oxide spacer, it is known[7] that there is some discrepancy between conformational energy values computed by the above semiempirical methods and those which achieve best agreement with experiments. So, the values adopted in the present study were estimated on the basis of (i) conformational energy calculations presently carried out and (ii) existing work[5–7,10,12] on polyoxyalkanes and similar chains. The energy minima and barrier heights in the pairs nonadjacent to the terephthalic group were recently used to investigate the local dynamics of polyoxyethylenes and were found to agree with NMR relaxation data.[13]

TABLE III. Results from calculations.[a]

	N_a	$-\dot{P}(a/a)\|_{t=0}$ (ns^{-1})	$P^{e}(a)$	λ_n (ns^{-1})	$\langle\tau\rangle$ (ns)
Series I					
$m = 1$	2	14.9	0.0014	0.021	47.6
2	72	18.9	0.046	0.911	1.05
3	30	50.1	0.0039	0.196	5.08
Series II					
$x = 3$	6	2.58	0.090	0.255	3.57
4	8	3.72	0.033	0.127	7.61
5	34	4.30	0.048	0.217	4.39
6	24	4.77	0.041	0.204	4.70

[a] The numbers of conformations in (ϕ_A) with nonzero equilibrium probabilities are denoted by N_a (Refs. 3 and 4). Only those excimer-forming states with equilibrium probability larger than 0.004 are considered for the polymer with $x = 6$.

B. Transition probabilities and mean first passage times

The numbers of conformations in $\{\phi\}_a$ are listed in Table III, based on the work of Mendicuti *et al.*[3,4] The transition probabilities for the stationary process for the passage from one macrostate to another are computed by combining the transition probabilities for the individual microstates in the macrostates. For instance, $P(a/a)$ is evaluated from

$$P(a/a) = \sum_{\phi_i} \sum_{\phi_j} P_{ij}^{(N)}(t) / \sum_{\phi_k} P_k^{(N)}(0), \tag{22}$$

where the summations are performed over conformations ϕ_i, ϕ_j, ϕ_k, all belonging to $\{\phi\}_a$. $P_{ij}^{(N)}(t)$ is the joint probability of occurrence of two conformations ϕ_i and ϕ_j with a time interval t, for a sequence of N mobile bonds, and $P_k^{(N)}(0)$ is the equilibrium probability of the k th conformation ϕ_k. $P_{ij}^{(N)}(t)$ are conveniently represented as the elements of the time-dependent joint probability matrix $P^{(N)}(t)$. The latter is evaluated according to the dynamic RIS model[8] from the stochastics of sequential pairs of bonds, relying on the assumption of pairwise dependent dynamics and statistics for the sequence. A brief description of the dynamic RIS model is presented in Sec. II of the preceding paper. For further details, the reader is referred to Ref. 8 and 13. $P_{ij}^{(N)}(t)$ may also be evaluated from the serial multiplication of stochastic weight matrices according to a mathemat-

TABLE II. Heights of saddles (kcal/mol)[a] Between the states $(\alpha\beta, \gamma\delta)$.

Segment	$(\alpha\beta, \gamma\delta)$					
	$(tt,tg^{\pm})$	$(tt,g^{\pm}t)$	$(g^{\pm}t,g^{\pm}g^{\pm})$	$(g^{\pm}g^{\pm},tg^{\pm})$	$(tg^{\pm},g^{\pm}g^{\pm})$	$(g^{\pm}g^{\pm},g^{\pm}t)$
1	3.2	9.6	3.7	9.6	9.6	3.7
2	3.1	9.0	3.5	8.8	9.2	6.4
3	3.1	3.1	2.7	3.0	3.0	2.7
4	3.7	9.8	4.0	9.0	12.0[b]	12.0
5	3.7	3.7	3.5	4.2	4.2	3.5
6	3.7	3.7	4.6	4.1	3.7	4.2
7	2.7	3.5	2.3	3.7	3.7	2.3
8	2.7	2.7	3.4	3.4	12.0	12.0
9	3.5	9.0	4.0	9.0	12.0	12.0

[a] All values are given with respect to the *tt* state whose conformational energy is set equal to zero.
[b] Barriers of 12 kcal/mol are taken instead of ∞, to avoid overflow.

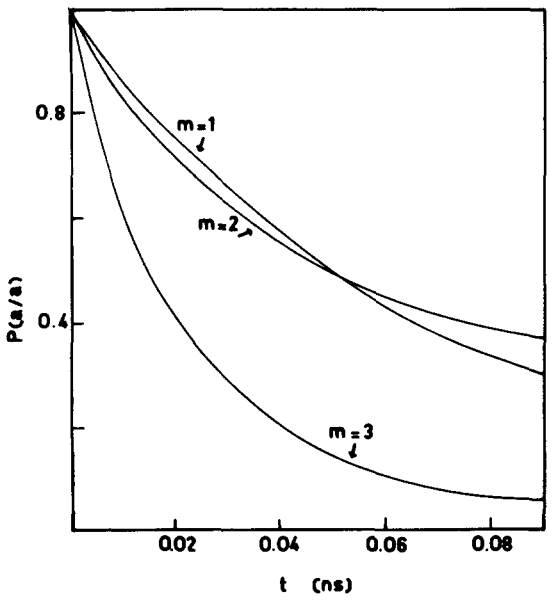

FIG. 9. Decay of transition probabilities $P(a/a)$ with time for the chains in series I, at 300 K. The dynamic RIS model with the data in Tables I and II has been used in calculations.

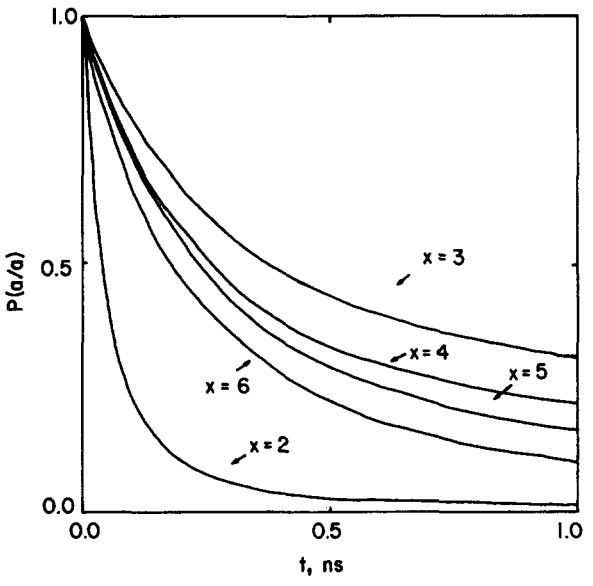

FIG. 10. Decay of the transition probabilities $P(a/a)$ with time for the chains in series II, at 300 K. The dynamic RIS model with the data in Tables I and II has been used in calculations.

ical method newly developed,[14] in analogy to the conventional matrix multiplication scheme[5] of equilibrium statistics.

The decays of $P(a/a)$ with time for the different members of series I and II are depicted in Figs. 9 and 10, respectively. The greater mobility of the oxyethylene segments is evident in the faster time scale for Fig. 9. Data in Tables I and II have been used to calculate the pair transition probabilities which are subsequently combined to evaluate $P_{ij}^{(N)}(t)$. The front factor A_0, which is inversely proportional to solvent viscosity,[1,8,13] was taken as 2.77×10^{11}/s for all polymeric chains. The initial slopes $\dot{P}(a/a)$ at $t=0$, the equilibrium probabilities $P^{\circ}(a)$ of macrostate $\{\phi\}_a$, the rate λ_n, and the mean first passage time $\langle\tau\rangle$ for each polymeric chain are listed in Table III. The increase with time in the fraction of sites suitable for excimer formation is displayed in Figs. 11(a) and 11(b), for the series I and II, respectively.

The curves in Figs. 11(a) and 11(b) are calculated from Eq. (11), where the rate constants λ_n are evaluated from the initial slopes of the transition probability curves in Figs. 9 and 10, according to Eq. (14). This approach is exact only if the decay of transition probabilities obeys a single exponential form. The same curves follow from Eq. (2) with $\mu=0$, provided that the single exponential decay is valid. However, inasmuch as several relaxational modes contribute to the orientational motion of the segments,[8,13] this approach is only approximate. Alternately, the best fitting parameters λ and μ which correspond to the decay curves in Figs. 9 and 10 may be evaluated from the time constant $(\lambda+\mu)^{-1}$ in Eq. (2) and knowledge of the equilibrium probabilities. The resulting λ values depend on the time window selected for curve fitting, and they approach λ_n as shorter time ranges are considered. Calculations show that the increase in the fraction of excimer-forming sites is relatively lower when best-fitting λ values are adopted, although the general qualitative features are conserved.

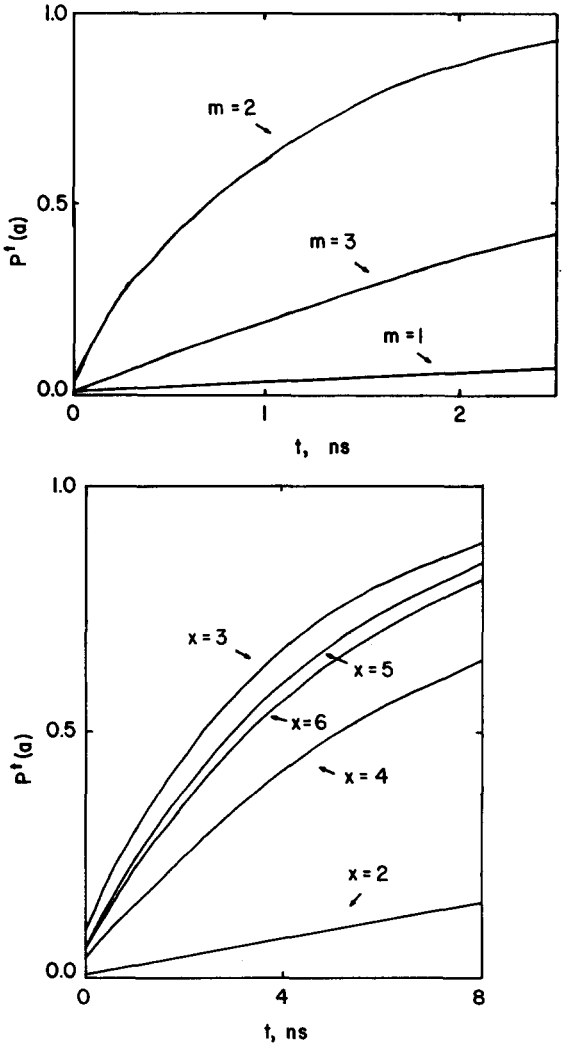

FIG. 11. Increase in the fraction of segments which has undergone transition to an excimer-forming conformation before time t, at $T=300$ K, for (a) the polymers in series I and (b) polymers in series II.

IV. RESULTS AND DISCUSSION

The mean first passage times resulting from calculations are in qualitative agreement with experiments. In series I, the highest excimer emission takes place in the case of the chain with $m = 2$.[3] As to the series II, an even–odd effect parallel to the one resulting from the present calculations is experimentally observed.[4]

From the examination of the curves in Figs. 9 and 10, it is clearly seen that the segments with a larger number of mobile bonds enjoy a higher freedom of motion. In fact, except for the shortest segment (whose behavior is dominated by the fact that the corresponding excimer-forming states are highly unstable), the decay of the transition probability $P(a/a)$ with time becomes faster as the chain length increases. That local motions are easier when a longer segment is allowed to move was also observed in previous studies[8,13,15] and attributed to the larger number of available paths for relaxation. Thus, the odd–even dependence of $\langle\tau\rangle$ or λ_n on the number of bonds between the aromatic groups does not originate from the contribution of local chain dynamics, but is prescribed instead by the equilibrium statistics of the chains. In fact, λ_n (or $\langle\tau\rangle$) values are governed by the static factor $P^\circ(a)/P^\circ(b)$ in Eq. (17), whose dependence on the specific chain investigated is much stronger than that of the dynamic factor $P(a/a)$ at $t = 0$. From the values tabulated in Table III, the dominant role of the equilibrium probabilities may be explicitly seen. Thus, it is not surprising that the experimentally observed behavior was recently rationalized[3,4] on the basis of equilibrium probabilities of excimer-forming states. In particular, it is interesting to note that, although the decays of the $P(a/a)$ curves for $m = 1$ and 2 (Fig. 9) are close to each other, the increase in the fraction $P'(a)$ of excimer-forming sites [Fig. 11(a)] is considerably faster for $m = 2$. The latter is due to the much higher equilibrium value $P^\circ(a)$ for $m = 2$ compared to $m = 1$, as apparent from the values listed in Table III.

Previous calculations indicate that static orientational correlations between two groups (or vectorial quantities) rigidly embedded in a chain, exhibit an odd–even dependence on the number of mobile bonds separating the two groups.[15] Thus, the observed behavior partly originates from that inherent characteristic of short polymeric segments, even though the process of excimer formation is restricted in the present case to the set of conformations leading to a cyclic structure. The dependence of dynamic correlations on the size of the mobile segment was not as pronounced as the static ones,[15] in accordance with the present results.

The present study shows that the analysis of the equilibrium probabilities of excimer-forming conformations may be satisfactorily employed for a preliminary qualitative estimation of the extent of excimer emission in a homologous series of chains. However, it is insufficient for a quantitative explanation unless the radiative lifetime of the excited monomer is very short. In general, the fraction of sites which will be traps for excimers continuously increases owing to conformational transitions, as displayed in Figs. 11(a) and 11(b). It should be recalled that for such diffusion controlled processes, the solvent viscosity plays an important role, as well. The effect of solvent viscosity is accounted for by the front factor A_0 in the dynamic RIS model. A_0 varies linearly with the reciprocal viscosity η^{-1}, according to the model. Such an inverse linear dependence between A_0 [or the instantaneous rates of conformational transitions from Eq. (6) in the preceding paper[1]] and the solvent viscosity has proven[13] to be a valid approach for treating local dynamics of polymers in dilute solution. Experiments by Cuniberti and Perico[16] also indicate that the intramolecular excimer to monomeric intensity ratio increases linearly with η^{-1}, provided that the thermodynamic power of the solvent is not significantly altered. An absolute value for A_0 for a specific polymer–solvent system is, in general, assigned through comparison with experiments. The value adopted in the present study is the one previously used for polyethylene[8] and polyoxyethylene solutions in solvents with a viscosity of about 1 cp.[13] The experiments by Mendicuti *et al*[3,4] were also carried out with solvents whose viscosities vary in the range $0.5 < \eta < 1.5$ cp, at room temperature.

The use of a constant value for A^0 corresponds to the approximation of the environmental effect on the motion by a mean frictional resistance for all types of mobile segments. The above treatment may be improved by considering the "size effect",[17] i.e., the increase in the frictional drag with the length of the path traveled by each moving unit during conformational transitions, by modifying the front factor A_0 according to the specific segment and transition considered. Inasmuch as this effect is not included in the present study, the results are representative of a limiting behavior for low viscosities.

Recent measurements[18] of the fluorescent lifetime of the model compound (dimethyl terephthalate) for the polymeric systems investigated, indicated that the latter is extremely short ($\sim$0.04 ns). The dynamic contribution to excimer emission from the part of sites created through conformational transitions is therefore small. For the chains in series I, with a higher degree of rotational mobility, part of the observed spectra may still originate from dynamic contribution, as may be concluded from the rapid increase, in Fig. 11(a), in the population of excimer-favoring sites. In fact, excimer fluorescence measurements in this series exhibit[19] a stronger sensitivity to solvent viscosity, in the direction predicted by chain dynamics. Experiments with chromophoric groups of longer fluorescent lifetime, in solvents of different viscosities but similar thermodynamic characteristics would furnish important information to realize the relative importance of the two factors in the investigated polymeric chains.

ACKNOWLEDGMENTS

This works was supported by National Science Foundation research Grant No. DMR 86-96071 and by a grant from the Exxon Education Foundation.

[1] I. Bahar and W. L. Mattice, J. Chem. Phys. **90**, 6775 (1989).
[2] H. Itagaki, K. Horie, I. Mita, M. Washio, S. Tagawa, Y. Tabata, H. Sato, and Y. Tanaka, Macromolecules **20**, 2774 (1987); F. C. de Schryver, L. Moens, M. van der Auweraer, N. Boens, L. Monnerie, and L. Bokobza, ibid. **17**, 1490 (1984).
[3] F. Mendicuti, V. N. Viswanadhan, and W. L. Mattice, Polymer **29**, 875 (1988).
[4] F. Mendicuti, B. Patel, V. N. Viswanadhan, and W. L. Mattice, Polymer **29**, 1669 (1988).

29, 1669 (1988).
[5]P. J. Flory, *Statistical Mechanics of Chain Molecules* (Interscience, New York, 1969).
[6]E. Riande, J. Polym. Sci., Polym. Phys. Ed. **15**, 1397 (1977); E. Riande and J. Guzmán, *ibid.* **23**, 1235 (1985).
[7]A. Abe and J. E. Mark, J. Am. Chem. Soc. **98**, 6468 (1976).
[8]I. Bahar and B. Erman, Macromolecules **20**, 1369 (1987).
[9]E. Parzen, *Stochastic Processes* (Holden-Day, San Francisco, 1962).
[10]E. Riande, J. G. de la Campa, D. D. Schlereth, J. Abajo, and J. Guzmán, Macromolecules **20**, 1641 (1987).
[11]K. S. Pitzer, Adv. Chem. Phys. **2**, 59 (1959).
[12]P. J. Flory and J. E. Mark, Makromol. Chem. **75**, 11 (1964); J. E. Mark and P. J. Flory, J. Am. Chem. Soc. **87**, 1415 (1966); **88**, 3702 (1966); A. Abe, J. W. Kennedy, and P. J. Flory, J. Polym. Sci. Polym. Phys. Ed. **14**, 1337 (1976); A. Abe, K. Tasaki, and J. E. Mark, Polym. J. **17**, 883 (1985); K. Tasaki and A. Abe, Polymer **17**, 641 (1985).
[13]I. Bahar, B. Erman, and L. Monnerie, Macromolecules **22**, 431 (1989).
[14]I. Bahar (work in progress).
[15]I. Bahar and B. Erman, J. Chem. Phys. **88**, 1228 (1988).
[16]C. Cuniberti and A. Perico, Eur. Polym. J. **16**, 887 (1980).
[17]I. Bahar, B. Erman, and L. Monnerie, Macromolecules (in press).
[18]F. Mendicuti, B. Patel, D. Waldeck, and W. L. Mattice, Polymer (in press).
[19]F. Mendicuti, B. Patel, and W. L. Mattice, Polymer (submitted).